Kybernetika

Jan Šembera; Jiří Maryška; Jiřina Královcová; Otto Severýn

A novel approach to modelling of flow in fractured porous medium

Kybernetika, Vol. 43 (2007), No. 4, 577--588

Persistent URL: `http://dml.cz/dmlcz/135798`

KYBERNETIKA — VOLUME *43* (2007), NUMBER 4, PAGES 577 – 588

A NOVEL APPROACH TO MODELLING OF FLOW IN FRACTURED POROUS MEDIUM

Jan Šembera, Jiří Maryška, Jiřina Královcová and Otto Severýn

There are many problems of groundwater flow in a disrupted rock massifs that should be modelled using numerical models. It can be done via "standard approaches" such as increase of the permeability of the porous medium to account the fracture system (or double-porosity models), or discrete stochastic fracture network models. Both of these approaches appear to have their constraints and limitations, which make them unsuitable for the large-scale long-time hydrogeological calculations. In the article, a new approach to the modelling of groudwater flow in fractured porous medium, which combines the above-mentioned models, is described. This article presents the mathematical formulation and demonstration of numerical results obtained by this new approach. The approach considers three substantial types of objects within a structure of modelled massif important for the groudwater flow – small stochastic fractures, large deterministic fractures, and lines of intersection of the large fractures. The systems of stochastic fractures are represented by blocks of porous medium with suitably set hydraulic conductivity. The large fractures are represented as polygons placed in 3D space and their intersections are represented by lines. Thus flow in 3D porous medium, flow in 2D and 1D fracture systems, and communication among these three systems are modelled together.

Keywords: finite element method, Darcy's flow, fractured porous medium

AMS Subject Classification: 86A05, 76M10

1. ROCK MASSIF ENVIRONMENT

Numerical modelling of the hydraulic, geochemical and transport processes in fractured rock attracts the attention of many scientists more than forty years. The first numerical models of such processes were created in late 1960's. According to [2], there existed more than thirty software packages claimed to solve problems of fluid flow in fractured rock in 1994.

Despite that fact, there is a lot of open and unresolved problems in this field of research. The reason for that lies in the nature of the problem – lack of input data, their uncertainty and often low accuracy, high computational cost are the main difficulties we encounter when we try to simulate processes in a fractured rock. It is possible to avoid these difficulties usually only at a price of simplification of the problem.

The hydrogeological research brought following empirical knowledge about the rock environment and groundwater flow in them:

- The rock matrix can be considered hydraulically impermeable.
- Even the most compact massifs are disrupted by numerous fractures.
- Most of the fractures are relatively small, with the characteristic length less than one meter.
- The groundwater flow in the small fractures has significant store capacity and play important role mainly in the transport processes.
- It is barely possible to obtain exact parameters of all the fractures, they should be treated in statistical way.
- The most of the liquid is conducted by relatively small number of large fractures. The spatial position of these fractures is usually detectable.
- The fastest groundwater flux is observed on intersections of the large fractures. These intersections behave like "pipelines" in the compact rock massifs.

These facts lead us to the conclusion that there are in general three different objects involved in conduction of the grounwater through a compact rock: small fractures, large fractures and intersections of large fractures.

There are two possible approaches to the modelling of flow in environment of *small fractures*: employment of the *stochastic discrete fracture networks* or the *homogenization and replacement with porous medium*. The first one is more suitable for small problems, see [7]. On the other hand the second approach is much better applicable for large problems. Fractured rock disrupted only by small fractures can by relatively well homogenized and replaced by hydraulically equivalent porous medium environment. The methods of homogenization and setting the hydraulic parameters of the porous medium can be found for example in [1].

The large fractures are relatively well known. The *discrete fracture network* approach works well in this case. Then, the fractures are represented as 2D objects (polygons) placed in 3D space.

The intersections of large fractures are relatively rare in the rock massifs, but significant for the flow. The velocity of the flow on the intersections of fractures can be higher in order of magnitude than velocity on the fractures. They can be represented by 1D objects placed in 3D space. Similar way can be represented also a possible borehole in the model.

On the base of our experience in groundwater flow modelling we decided to build up a model that could treat all the above–mentioned objects. The model incorporates 3D blocks, considered as porous medium, 2D fractures, standing for real rock fractures, and 1D lines, representing significant pipelines in the underground.

2. LINEAR STEADY DARCY FLOW

In general, the linear steady Darcy flow, which we expect in a considered underground domain, is described by the equations

$$\boldsymbol{u} = -\boldsymbol{K}\,\nabla p, \tag{1}$$

$$\nabla\cdot\boldsymbol{u} = q\,, \tag{2}$$

where $\boldsymbol{u}$ is the vector of Darcy velocity of the flow, p is the hydraulic pressure, $\boldsymbol{K}$ is the second order tensor of hydraulic conductivity (symmetric, positive definite), and q is a function expressing the density of sources or sinks of the fluid.

The equation (1) is the Darcy's law – the relation between pressure and water velocity in porous medium. The equation (2) is the equation of continuity. Sources q usually represent injection or pumping out the water from the porous medium.

The steady Darcy flow problem is governed by these two equations and it is solved in a bounded region (1D, 2D, or 3D) with boundary conditions generally of three sorts. For setting the problem correctly, it is necessary to prescribe a Dirichlet boundary condition

$$p = p_D,$$

which determines water pressure on one part of the boundary. On the resting part of boundary, the Neumann boundary condition prescribing water flow through the boundary

$$\boldsymbol{u} \cdot \boldsymbol{n} = u_N$$

(where $\boldsymbol{n}$ is outer boundary normal vector) or more general Newton boundary condition

$$\boldsymbol{u} \cdot \boldsymbol{n} - \sigma_N (p - p_N) = 0$$

can be prescribed.

3. MATHEMATICAL FORMULATION OF THE PROBLEM

Let us consider three domains Ω_3, Ω_2 and Ω_1, $\Omega_3 \subset R^3$, $\Omega_2 \subset R^3$, $\Omega_1 \subset R^3$. Besides let Ω_3 be a simply connected three dimensional polyhedral domain, Ω_2 be a finite set of mutually connected polygons placed in 3D space and Ω_1 be a finite set of mutually connected line segments placed in 3D space.

Let the boundary of each domain be divided into two parts – Dirichlet part and Neumann part: Boundary of domain Ω_3: $\partial\Omega_3 = \Gamma_{3,D} \cup \Gamma_{3,N}$, $\Gamma_{3,D} \neq \emptyset$, $\Gamma_{3,D} \cap \Gamma_{3,N} = \emptyset$. Boundary of domain Ω_2: $\partial\Omega_2 = \Gamma_{2,D} \cup \Gamma_{2,N}$, $\Gamma_{2,D} \neq \emptyset$, $\Gamma_{2,D} \cap \Gamma_{2,N} = \emptyset$ and Boundary of domain Ω_1: $\partial\Omega_1 = \Gamma_{1,D} \cup \Gamma_{1,N}$, $\Gamma_{1,D} \neq \emptyset$, $\Gamma_{1,D} \cap \Gamma_{1,N} = \emptyset$. ($\partial\Omega_1$ is a set of discrete points).

The potential driven flow in the domain Ω_i $(i = 1, 2, 3)$ can be described by the following system of equations:

$$\begin{aligned}
\boldsymbol{u}_i &= -\boldsymbol{K}_i \nabla p_i && \text{in} \quad \Omega_i, && (3)\\
\nabla \cdot \boldsymbol{u}_i &= q_i + \tilde{q}_{\langle i+1\rangle,i} + \tilde{q}_{\langle i+2\rangle,i} && \text{in} \quad \Omega_i, && (4)\\
p_i &= p_{i,D} && \text{on} \quad \Gamma_{i,D}, && (5)\\
\boldsymbol{u}_i \cdot \boldsymbol{n} &= u_{i,N} && \text{on} \quad \Gamma_{i,N}, && (6)
\end{aligned}$$

where $\langle i+1\rangle$, $\langle i+2\rangle$ stand for $(i \bmod 3) + 1$, $(i + 1 \bmod 3) + 1$ respectively.

The flow between two different domains is considered as a positive or negative source of fluid $\tilde{q}_{i,j}$. Its properties follow:

$$\begin{aligned}
\tilde{q}_{i,j} &= (p_i - p_j)\sigma_{ij}\,, \quad i \neq j,\\
\sigma_{ij} &= 0 \quad \text{in} \quad (\Omega_i \cup \Omega_j) \setminus (\Omega_i \cap \Omega_j),
\end{aligned}$$

The quantity σ_{ij} stands for the permeability between domains Ω_i and Ω_j. $\sigma_{ij} = \sigma_{ji}$ so $\tilde{q}_{ij} = -\tilde{q}_{ji}$.

The unknowns of the problem are the values of physical quantities p_i, $\boldsymbol{u}_i$ $(i = 1, 2, 3)$ over the considered domains. The problem parameters are the domains Ω_i, their boundaries $\Gamma_{i,D}$ and $\Gamma_{i,N}$, values of boundary conditions $p_{i,D}$, $u_{i,N}$ $(i = 1, 2, 3)$, and values of material parameters $\boldsymbol{K}_i$, σ_{ij} $(i, j = 1, 2, 3,\ i \neq j)$.

4. MIXED–HYBRID FORMULATION

Let us consider three domains with their boundaries as it was mentioned above. Let us define the discretization of each domain into a set of subdomains, denote $\tau_{i,h}$ the partition of the domain Ω_i $(i = 1, 2, 3)$, i. e.

$$\begin{aligned}
\tau_{3,h} &= \{e; e \in \Omega_3, \cup_{e\in\tau_{3,h}} \bar{e} = \Omega_3, e_i \cap e_j = \emptyset \text{ for } i \neq j\},\\
\tau_{2,h} &= \{e; e \in \Omega_2, \cup_{e\in\tau_{2,h}} \bar{e} = \Omega_2, e_i \cap e_j = \emptyset \text{ for } i \neq j\},\\
\tau_{1,h} &= \{e; e \in \Omega_1, \cup_{e\in\tau_{1,h}} \bar{e} = \Omega_1, e_i \cap e_j = \emptyset \text{ for } i \neq j\}.
\end{aligned}$$

Let us denote $\Gamma_{i,h}$ the sets of points on all nondirichlet faces in each domain:

$$\begin{aligned}
\Gamma_{3,h} &= \cup_{e\in\tau_{3,h}} \partial e \setminus \Gamma_{3,D},\\
\Gamma_{2,h} &= \cup_{e\in\tau_{2,h}} \partial e \setminus \Gamma_{2,D},\\
\Gamma_{1,h} &= \cup_{e\in\tau_{1,h}} \partial e \setminus \Gamma_{1,D}.
\end{aligned}$$

Let us emphasize the fact that no special demands for the mutual position of subdomains of different dimensions are prescribed.

For each $\Omega \in \{\Omega_1, \Omega_2, \Omega_3\}$, $\Gamma_h \in \{\Gamma_{1,h}, \Gamma_{2,h}, \Gamma_{3,h}\}$, $\tau_h \in \{\tau_{1,h}, \tau_{2,h}, \tau_{3,h}\}$ we use the following function spaces: The standard space of square-integrable functions $L^2(\Omega)$, the standard Sobolev space of scalar functions with square-integrable weak derivatives $H^1(\Omega)$, the space $H^{\frac{1}{2}}(\Gamma_h)$ of functions being trace of a function of corresponding $H^1(\Omega)$. For each subdomain $e \in \tau_h$, let us denote by $\boldsymbol{H}(div, e)$ the space of vector functions with square–integrable weak divergences and define $\boldsymbol{H}(div, \tau_h)$ as the space of functions from $\boldsymbol{L}^2(\Omega)$ whose restriction to each subdomain $e \in \tau_h$ lies in $\boldsymbol{H}(div, e)$.

In the following expressions β denotes the inverse of $\boldsymbol{K}$, i. e. hydraulic resistance, f^e denotes the restriction of function f on subdomain e, $(f, g)_e$ denotes the $L^2(e)$ scalar product of f and g, i. e. $\int_e fg\,\mathrm{d}x$, and $\langle f, g\rangle_{\partial e}$ denotes the integral form $\int_{\partial e} fg\,\mathrm{d}x$.

Let $\boldsymbol{u}_3 \in \boldsymbol{C}^1(\Omega_3)$ (a vector function with continuous derivatives of the first order) and $p_3 \in C(\Omega_3)$ (a continuous scalar function) fulfill the equations (3)–(6). Considering a particular subdomain $e \in \tau_{3,h}$, the following equations obviously hold:

$$\begin{aligned}
\beta_3^e \boldsymbol{u}_3^e + \nabla p_3^e &= 0,\\
\nabla \cdot \boldsymbol{u}_3^e - \tilde{q}_{23}^e - \tilde{q}_{13}^e &= q_3^e.
\end{aligned}$$

Multiplying the first equation by any test function $\boldsymbol{v}_3 \in \boldsymbol{H}(div, \tau_{3,h})$ and the second one by another test function $\phi_3 \in L^2(\Omega_3)$ and integrating over e we obtain

$$\begin{aligned}
(\beta_3^e \boldsymbol{u}_3^e, \boldsymbol{v}_3^e)_e + (\nabla p_3^e, \boldsymbol{v}_3^e)_e &= 0,\\
(\nabla \cdot \boldsymbol{u}_3^e, \phi_3^e)_e - ((p_2^e - p_3^e)\sigma_{23}^e, \phi_3^e)_e - ((p_1^e - p_3^e)\sigma_{13}^e, \phi_3^e)_e &= (q_3^e, \phi_3^e)_e\,.
\end{aligned}$$

Let us denote ψ_3^e the restriction of continuous function p_3^e to ∂e. Applying the Green's formula the equalities can be read as

$$\begin{array}{rcl} (\beta_3^e \boldsymbol{u}_3^e, \boldsymbol{v}_3^e)_e - (p_3^e, \nabla\cdot \boldsymbol{v}_3^e)_e + \langle \psi_3^e, \boldsymbol{v}_3^e \cdot \boldsymbol{n}^e \rangle_{\partial e} & = & 0, \\ (\nabla \cdot \boldsymbol{u}_3^e, \phi_3^e)_e - ((p_2^e - p_3^e)\sigma_{23}^e, \phi_3^e)_e - ((p_1^e - p_3^e)\sigma_{13}^e, \phi_3^e)_e & = & (q_3^e, \phi_3^e)_e \,, \end{array}$$

where $\boldsymbol{n}^e$ stands for outer normal of ∂e.

Summing the above equalities over all subdomains of $\tau_{3,h}$ we get

$$\sum_{e\in\tau_{3,h}} \{(\beta_3^e \boldsymbol{u}_3^e, \boldsymbol{v}_3^e)_e - (p_3^e, \nabla\cdot \boldsymbol{v}_3^e)_e + \langle \psi_3^e, \boldsymbol{v}_3^e \cdot \boldsymbol{n}^e \rangle_{\partial e}\} = 0$$

$$\sum_{e\in\tau_{3,h}} \{(\nabla \cdot \boldsymbol{u}_3^e, \phi_3^e)_e - ((p_2^e - p_3^e)\sigma_{23}^e, \phi_3^e)_e - ((p_1^e - p_3^e)\sigma_{13}^e, \phi_3^e)_e\} = \sum_{e\in\tau_{3,h}} (q_3^e, \phi_3^e)_e.$$

Extra equations expressing the continuity of $\boldsymbol{u}_3$ on internal faces between neighbouring subdomains of $\tau_{3,h}$ have to hold, too. The continuity on the face iterconnecting subdomains e_k and e_l can be written down as

$$\boldsymbol{u}_3^{e_k} \cdot \boldsymbol{n}^{e_k} + \boldsymbol{u}_3^{e_l} \cdot \boldsymbol{n}^{e_l} = 0.$$

Let us test the equation by any function $\mu_3 \in H^{\frac{1}{2}}(\Gamma_{3,h})$ and sum over all internal faces of partition $\tau_{3,h}$:

$$\sum_{e\in\tau_{3,h}} \langle \boldsymbol{u}_3^e \cdot \boldsymbol{n}^e, \mu_3^e \rangle_{\partial e \cap (\Gamma_{3,h} \setminus \Gamma_{3,N})} = 0.$$

Changing the sign of the balance equation and introducing the boundary conditions, the following system of integral equations on partition $\tau_{3,h}$ can be derived:

$$\sum_{e\in\tau_{3,h}} \left\{(\beta_3^e \boldsymbol{u}_3^e, \boldsymbol{v}_3^e)_e - (p_3^e, \nabla\cdot \boldsymbol{v}_3^e)_e + \langle \psi_3^e, \boldsymbol{v}_3^e \cdot \boldsymbol{n}^e \rangle_{\partial e\cap\Gamma_{3,h}}\right\}$$
$$= - \sum_{e\in\tau_{3,h}} \langle p_{3,D}, \boldsymbol{v}_3^e \cdot \boldsymbol{n}^e \rangle_{\partial e\cap\Gamma_{3,D}}, \tag{7}$$

$$\sum_{e\in\tau_{3,h}} \{-(\nabla \cdot \boldsymbol{u}_3^e, \phi_3^e)_e + ((p_{23}^e - p_3^e)\sigma_{23}^e, \phi_3^e)_e + ((p_{13}^e - p_3^e)\sigma_{13}^e, \phi_3^e)_e\}$$
$$= - \sum_{e\in\tau_{3,h}} (q_3^e, \phi_3^e)_e, \tag{8}$$

$$\sum_{e\in\tau_{3,h}} \langle \boldsymbol{u}_3^e \cdot \boldsymbol{n}^e, \mu_3^e \rangle_{\partial e\cap\Gamma_{3,h}} = \sum_{e\in\tau_{3,h}} \langle u_{3,N}^e, \mu_3^e \rangle_{\partial e\cap\Gamma_{3,N}}. \tag{9}$$

The same way can be derived the system of integral equations on partitions $\tau_{2,h}$ and $\tau_{1,h}$:

$$\sum_{e\in\tau_{2,h}} \left\{(\beta_2^e \boldsymbol{u}_2^e, \boldsymbol{v}_2^e)_e - (p_2^e, \nabla\cdot \boldsymbol{v}_2^e)_e + \langle \psi_2^e, \boldsymbol{v}_2^e \cdot \boldsymbol{n}^e \rangle_{\partial e\cap\Gamma_{2,h}}\right\}$$

$$= - \sum_{e\in\tau_{2,h}} \langle p_{2,D}, \boldsymbol{v}_2^e \cdot \boldsymbol{n}^e \rangle_{\partial e\cap\Gamma_{2,D}}, \tag{10}$$

$$\sum_{e\in\tau_{2,h}} \{-(\nabla\cdot \boldsymbol{u}_2^e, \phi_2^e)_e + ((p_{32}^e - p_2^e)\sigma_{32}^e, \phi_2^e)_e + ((p_{12}^e - p_2^e)\sigma_{12}^e, \phi_2^e)_e\}$$

$$= - \sum_{e\in\tau_{2,h}} (q_2^e, \phi_2^e)_e, \tag{11}$$

$$\sum_{e\in\tau_{2,h}} \langle \boldsymbol{u}_2^e \cdot \boldsymbol{n}^e, \mu_2^e \rangle_{\partial e\cap\Gamma_{2,h}} = \sum_{e\in\tau_{2,h}} \langle u_{2,N}^e, \mu_2^e \rangle_{\partial e\cap\Gamma_{2,N}}, \tag{12}$$

$$\sum_{e\in\tau_{1,h}} \left\{(\beta_1^e u_1^e, v_1^e)_e - (p_1^e, v_1^{e\prime})_e + \langle \psi_1^e, v_1^e \cdot n^e \rangle_{\partial e\cap\Gamma_{1,h}}\right\}$$

$$= - \sum_{e\in\tau_{1,h}} \langle p_{1,D}, v_1^e \cdot n^e \rangle_{\partial e\cap\Gamma_{1,D}}, \tag{13}$$

$$\sum_{e\in\tau_{1,h}} \left\{-(u_1^{e\prime}, \phi_1^e)_e + ((p_{31}^e - p_1^e)\sigma_{31}^e, \phi_1^e)_e + ((p_{21}^e - p_1^e)\sigma_{21}^e, \phi_1^e)_e\right\}$$

$$= - \sum_{e\in\tau_{1,h}} (q_1^e, \phi_1^e)_e, \tag{14}$$

$$\sum_{e\in\tau_{1,h}} \langle u_1^e \cdot n^e, \mu_1^e \rangle_{\partial e\cap\Gamma_{1,h}} = \sum_{e\in\tau_{1,h}} \langle u_{1,N}^e, \mu_1^e \rangle_{\partial e\cap\Gamma_{1,N}}, \tag{15}$$

where $'$ means the first derivative and n^e is outer normal in 1D, i. e. either $+1$ or -1.

In the equations (8), (11), (14) the functions $p_{ij}^{e_j}$ for $e_j \in \tau_{j,h}$, $i \neq j$, $i, j \in \{1, 2, 3\}$ stand for

$$\sum_{e_i\in\tau_{i,h}} p_{ij}^{e_i,e_j}, \tag{16}$$

where $p_{ij}^{e_i,e_j}$ are any functions fulfilling the following conditions:

$$\text{for } i < j: \quad p_{ij}^{e_i,e_j} \in L^2(e_j): \quad \int_{e_j} p_{ij}^{e_i,e_j}\,\mathrm{d}x = \int_{e_i\cap e_j} p_i\,\mathrm{d}x, \tag{17}$$

$$\text{for } i > j: \; p_{ij}^{e_i,e_j} \in L^2(e_i \cap e_j): \int_{e_i\cap e_j} p_{ij}^{e_i,e_j}\,\mathrm{d}x = \frac{|e_i\cap e_j|_j}{|e_i|_i} \int_{e_i} p_i\,\mathrm{d}x, \tag{18}$$

where $|e|_i$ means the i-dimensional measure of e.

Next introduce the function space (Z):

$$\begin{aligned}\boldsymbol{Z} \;\; = \;\; & \boldsymbol{H}(div, \tau_{3,h}) \times \boldsymbol{H}(div, \tau_{2,h}) \times \boldsymbol{H}(div, \tau_{1,h}) \\ & \times L^2(\tau_{3,h}) \times L^2(\tau_{2,h}) \times L^2(\tau_{1,h}) \times H^{\frac{1}{2}}(\Gamma_{3,h}) \times H^{\frac{1}{2}}(\Gamma_{2,h}) \times H^{\frac{1}{2}}(\Gamma_{2,h}).\end{aligned}$$

Definition 1. We call the function

$$\bar{\boldsymbol{z}} = (\boldsymbol{u}_3, \boldsymbol{u}_2, \boldsymbol{u}_1, p_3, p_2, p_1, \psi_3, \psi_2, \psi_1) \in \boldsymbol{Z}$$

the weak solution of mixed hybrid formulation of the problem of flow in fracture porous medium, if for all functions

$$\boldsymbol{z} = (\boldsymbol{v}_3, \boldsymbol{v}_2, \boldsymbol{v}_1, \varphi_3, \varphi_2, \varphi_1, \mu_3, \mu_2, \mu_1) \in \boldsymbol{Z}$$

$\bar{\boldsymbol{z}}$ satisfies the equations (7)–(15).

5. FINITE ELEMENT APPROXIMATION

We are using the same approximation as [5]. Let $\tau_{3,h}$ be a partition of Ω_3 into simplex elements, $\tau_{2,h}$ be a partition of Ω_2 into triangle elements and $\tau_{1,h}$ be a partition of Ω_1 into line elements.

For the approximation of function spaces $\boldsymbol{H}(div, \tau_{i,h})$ we use the Raviart–Thomas spaces of piecewise linear functions $\mathbf{RT}^0_{-1}(\tau_{i,h}) = \{\boldsymbol{f} \in \boldsymbol{L}^2(\Omega_i) | (\forall e \in \tau_{i,h})(\boldsymbol{f}^e \in \mathbf{RT}^0(e))\}$ $(i = 1, 2, 3)$. The local Raviart–Thomas spaces $\mathbf{RT}^0(e)$ are defined in each dimension a different way:

- in 3D (for $e \in \tau_{3,h}$): $\mathbf{RT}^0(e) = \mathrm{span}\{\boldsymbol{v}^e_{3,i} | i \in \{1, 2, 3, 4\}\}$, where

  $$\boldsymbol{v}^e_{3i}(\boldsymbol{x}) = k \begin{pmatrix} x - \alpha \\ y - \beta \\ z - \gamma \end{pmatrix},$$

  parameters k, α, β, and γ are chosen so that

  $$\int_{f^e_{3j}} \boldsymbol{v}_{3i} \cdot \boldsymbol{n}_{3j} = \delta_{ij} \ , \quad i, j \in \{1, 2, 3, 4\},$$

  where f^e_{3j} $(j = 1, 2, 3, 4)$ are individual faces of the tetrahedron e, $\boldsymbol{n}_{3j}$ is the outward normal vector of the face f^e_{3j} and δ_{ij} is the Kronecker symbol.

- in 2D (for $e \in \tau_{2,h}$): $\mathbf{RT}^0(e) = \mathrm{span}\{\boldsymbol{v}^e_{2,i} | i \in \{1, 2, 3\}\}$, where

  $$\boldsymbol{v}^e_{2i}(\boldsymbol{x}) = k \begin{pmatrix} x - \alpha \\ y - \beta \end{pmatrix},$$

  parameters k, α, and β are chosen so that

  $$\int_{f^e_{2j}} \boldsymbol{v}_{2i} \cdot \boldsymbol{n}_{2j} = \delta_{ij} \ , \quad i, j \in \{1, 2, 3\},$$

  where f^e_{2j} $(j = 1, 2, 3)$ are individual edges of the triangle e and $\boldsymbol{n}_{2j}$ is the outward normal vector of the edge f^e_{2j}.

- in 1D (for $e \in \tau_{1,h}$): $\mathbf{RT}^0(e) = P_1(e)$ (the space of all linear function on e).

For the approximation of function spaces $L^2(\tau_{i,h})$ we use the multiplicator spaces of piecewise constant functions $M^0_{-1}(\tau_{i,h}) = \mathrm{span}\{\phi^e | e \in \tau_{i,h}\}$ $(i = 1, 2, 3)$, where $\phi^e(\boldsymbol{x}) = 1$ for $x \in e$ and $\phi^e(\boldsymbol{x}) = 0$ otherwise.

For the approximation of function spaces $H^{\frac{1}{2}}(\Gamma_{i,h})$ we use the multiplicator spaces of piecewise constant functions $M^0_{-1}(\Gamma_{i,h}) = \mathrm{span}\{\Psi^f | f \in \Gamma_{i,h}\}$ $(i = 1, 2, 3)$, where $\Psi^f(\boldsymbol{x}) = 1$ for $x \in f$ and $\Psi^f(\boldsymbol{x}) = 0$ otherwise.

For more details about the approximation function spaces, see e. g. [3].

Let us define the approximation space

$$\begin{aligned}\tilde{\boldsymbol{Z}} &= \mathbf{RT}^0_{-1}(\tau_{3,h}) \times \mathbf{RT}^0_{-1}(\tau_{2,h}) \times \mathbf{RT}^0_{-1}(\tau_{1,h}) \\ &\quad \times M^0_{-1}(\tau_{3,h}) \times M^0_{-1}(\tau_{2,h}) \times M^0_{-1}(\tau_{1,h}) \times M^0_{-1}(\Gamma_{3,h}) \times M^0_{-1}(\Gamma_{2,h}) \times M^0_{-1}(\Gamma_{1,h})\end{aligned}$$

and approximate the function $\bar{\boldsymbol{z}} = (\boldsymbol{u}_3, \boldsymbol{u}_2, \boldsymbol{u}_1, p_3, p_2, p_1, \psi_3, \psi_2, \psi_1) \in \boldsymbol{Z}$ and test function $\boldsymbol{z} = (\boldsymbol{v}_3, \boldsymbol{v}_2, \boldsymbol{v}_1, \phi_3, \phi_2, \phi_1, \mu_3, \mu_2, \mu_1) \in \boldsymbol{Z}$ by the functions $\tilde{\bar{\boldsymbol{z}}} = (\tilde{\boldsymbol{u}}_3, \tilde{\boldsymbol{u}}_2, \tilde{\boldsymbol{u}}_1, \tilde{p}_3, \tilde{p}_2, \tilde{p}_1, \tilde{\psi}_3, \tilde{\psi}_2, \tilde{\psi}_1) \in \tilde{\boldsymbol{Z}}$ and $\tilde{\boldsymbol{z}} = (\tilde{\boldsymbol{v}}_3, \tilde{\boldsymbol{v}}_2, \tilde{\boldsymbol{v}}_1, \tilde{\phi}_3, \tilde{\phi}_2, \tilde{\phi}_1, \tilde{\mu}_3, \tilde{\mu}_2, \tilde{\mu}_1) \in \tilde{\boldsymbol{Z}}$ respectively.

Formal evaluating the equations (7)–(15) for the proposed function and test function approximations leads to the following system:

$$\begin{aligned} & \sum_{e\in\tau_{i,h}} \Big\{ (\beta_i^e \tilde{\boldsymbol{u}}_i^e, \tilde{\boldsymbol{v}}_i^e)_e - (\tilde{p}_i^e, \nabla\cdot\tilde{\boldsymbol{v}}_i^e)_e + \langle \tilde{\psi}_i^e, \tilde{\boldsymbol{v}}_i^e \cdot \boldsymbol{n}^e\rangle_{\partial e\cap\Gamma_{i,h}} \Big\} \\ = & \; - \sum_{e\in\tau_{i,h}} \langle p_{i,D}, \tilde{\boldsymbol{v}}_i^e \cdot \boldsymbol{n}^e \rangle_{\partial e\cap\Gamma_{i,D}}, \end{aligned} \tag{19}$$

$$\begin{aligned} & \sum_{e\in\tau_{i,h}} \Big\{ -(\nabla\cdot\tilde{\boldsymbol{u}}_i^e, \tilde{\phi}_i^e)_e + ((\tilde{p}^e_{\langle i+1\rangle,i} - \tilde{p}_i^e)\sigma^e_{\langle i+1\rangle,i}, \tilde{\phi}_i^e)_e \\ & \qquad + ((\tilde{p}^e_{\langle i+2\rangle,i} - \tilde{p}_i^e)\sigma^e_{\langle i+2\rangle,i}, \tilde{\phi}_i^e)_e \Big\} = - \sum_{e\in\tau_{i,h}} (q_i^e, \tilde{\phi}_i^e)_e, \end{aligned} \tag{20}$$

$$\sum_{e\in\tau_{i,h}} \langle \tilde{\boldsymbol{u}_i^e} \cdot \boldsymbol{n}^e, \tilde{\mu}_i^e \rangle_{\partial e\cap\Gamma_{i,h}} = \sum_{e\in\tau_{i,h}} \langle u^e_{i,N}, \tilde{\mu}_i^e\rangle_{\partial e\cap\Gamma_{i,N}}. \tag{21}$$

Here the meaning of $\tilde{p}^e_{i+1,i}$ and $\tilde{p}^e_{i+2,i}$ is analogical to (16)–(18) considering shortened notation of $(i \bmod 3) + 1$ as $\langle i+1\rangle$ and $(i+1 \bmod 3) + 1$ as $\langle i+2\rangle$.

Definition 2. We call the function $\tilde{\bar{\boldsymbol{z}}} = (\tilde{\boldsymbol{u}}_3, \tilde{\boldsymbol{u}}_2, \tilde{\boldsymbol{u}}_1, \tilde{p}_3, \tilde{p}_2, \tilde{p}_1, \tilde{\psi}_3, \tilde{\psi}_2, \tilde{\psi}_1) \in \tilde{\boldsymbol{Z}}$ the mixed-hybrid finite element approximation of the weak solution of the problem of flow in fracture porous medium, if for all functions $\tilde{\boldsymbol{z}} = (\tilde{\boldsymbol{v}}_3, \tilde{\boldsymbol{v}}_2, \tilde{\boldsymbol{v}}_1, \tilde{\phi}_3, \tilde{\phi}_2, \tilde{\phi}_1, \tilde{\mu}_3, \tilde{\mu}_2, \tilde{\mu}_1) \in \tilde{\boldsymbol{Z}}$ the the equations (19)–(21) hold for $i \in \{1, 2, 3\}$.

Let us use the following notation for the partial functions of $\tilde{\bar{\mathbf{z}}}$ $(i = 1, 2, 3)$:

$$\begin{aligned} \tilde{\boldsymbol{u}}_i &= \sum_{e\in\tau_{i,h}} \sum_{j\in I_i} V_{ij}^e \boldsymbol{v}_{3j}^e, & I_1 &= \{1,2\},\; I_2 = \{1,2,3\},\; I_3 = \{1,2,3,4\}, \\ \tilde{p}_i &= \sum_{e\in\tau_{i,h}} P_i^e \phi^e, & \tilde{\psi}_i &= \sum_{f\in\Gamma_{i,h}} \mu_i^f \Psi^f \end{aligned}$$

Obviously, it is sufficient to evaluate the equations (19)–(21) only for all test functions chosen from the basis of $\tilde{\boldsymbol{Z}}$, i. e. for the following sets $(i = 1, 2, 3)$:

$$\tilde{\boldsymbol{v}}_i \in \{\boldsymbol{v}_{ij}^e | e \in \tau_{i,h}, j \in I_i\}, \qquad \tilde{\phi}_i \in \{\phi^e | e \in \tau_{i,h}\}, \qquad \tilde{\mu}_i \in \{\Psi^f | f \in \Gamma_{i,h}\}$$

Let us order the elements of $\tau_{i,h}$ and faces of $\Gamma_{i,h}$ and align the unknown coefficients into vectors the following way ($i = 1, 2, 3$):

$$\begin{aligned}
\boldsymbol{V}_i &= (V_{i1}^{e_1}, V_{i2}^{e_1}, V_{i3}^{e_1}, V_{i4}^{e_1}, V_{i1}^{e_2}, \dots)^T, \\
\boldsymbol{P}_i &= (P_i^{e_1}, P_i^{e_2}, P_i^{e_3}, \dots)^T, \\
\boldsymbol{\Psi}_i &= (\mu_i^{f_1}, \mu_i^{f_2}, \mu_i^{f_3}, \dots)^T.
\end{aligned}$$

The system (19)–(21) then converts to the following system of linear algebraic equations:

$$\begin{array}{llllllllllll}
\mathring{A}_3\boldsymbol{V}_3 & & & +\boldsymbol{B}_3\boldsymbol{P}_3 & & & +\boldsymbol{C}_3\boldsymbol{\Psi}_3 & & & = & \boldsymbol{q}_{3D} \\
& \mathring{A}_2\boldsymbol{V}_2 & & & +\boldsymbol{B}_2\boldsymbol{P}_2 & & & +\boldsymbol{C}_2\boldsymbol{\Psi}_2 & & = & \boldsymbol{q}_{2D} \\
& & \mathring{A}_1\boldsymbol{V}_1 & & & +\boldsymbol{B}_1\boldsymbol{P}_1 & & & +\boldsymbol{C}_1\boldsymbol{\Psi}_1 & = & \boldsymbol{q}_{1D} \\
\boldsymbol{B}_3^T\boldsymbol{V}_3 & & & +\boldsymbol{D}_3\boldsymbol{P}_3 & +\boldsymbol{D}_{32}\boldsymbol{P}_2 & +\boldsymbol{D}_{31}\boldsymbol{P}_1 & & & & = & \boldsymbol{q}_{3E} \\
& \boldsymbol{B}_2^T\boldsymbol{V}_2 & & +\boldsymbol{D}_{32}^T\boldsymbol{P}_3 & +\boldsymbol{D}_2\boldsymbol{P}_2 & +\boldsymbol{D}_{21}\boldsymbol{P}_1 & & & & = & \boldsymbol{q}_{2E} \\
& & \boldsymbol{B}_3^T\boldsymbol{V}_1 & +\boldsymbol{D}_{31}^T\boldsymbol{P}_3 & +\boldsymbol{D}_{21}^T\boldsymbol{P}_2 & +\boldsymbol{D}_1\boldsymbol{P}_1 & & & & = & \boldsymbol{q}_{1E} \\
\boldsymbol{C}_3^T\boldsymbol{V}_3 & & & & & & & & & = & \boldsymbol{q}_{3N} \\
& \boldsymbol{C}_2^T\boldsymbol{V}_2 & & & & & & & & = & \boldsymbol{q}_{2N} \\
& & \boldsymbol{C}_1^T\boldsymbol{V}_1 & & & & & & & = & \boldsymbol{q}_{1N}
\end{array} ,$$

The resulting system matrix is symmetric, sparse of characteristic internal structure, indefinite. The blocks $\mathring{A}_i$ are positive definite. The properties enable to use specialized solvers of linear equation systems (see [6]) to make the process of solving more effective.

The well-posedness and convergence of the method to the weak solution was studied for partial problems in [4] (only 3D problem) and [8] (only 2D fractures in 3D). The complete 1D-2D-3D problem as set here was not theoretically studied, yet.

6. NUMERICAL EXAMPLE

The proposed approach to modelling of flow in fractured medium was implemented and a simple test problem was set up to see the effect of inclusion of fractures into porous medium model. Two hydraulically equivalent models of one small area were built. The first one is a model of the polygonal area with two intersecting fractures. The shape of the area and position of the fractures can be seen at Figure 1. The dimensions in plan-view are about 10×10 km, the depth is 900 m. The area is slightly slanted in y-axes direction – the vertical distance is 50 m. The area is composed of five geological layers. The upper one is 100 m deep, the depth of each of the other ones is 200 m. The permeability of each layer is homogeneous and isotropic. The values of layers' permeability are from top to bottom respectively 100, 10, 50, 0.001, and 0.5 m/day. The permeability of fractures is homogeneous and isotropic, its value is $3{*}10^5$ m/day. The inter-dimensional permeability σ_{23} was set equal to 1 in whole fracture system.

The boundary conditions on upper and lower parts of the boundary of both the 3D area and the 2D fracture system, such as at the left and right parts (in view of

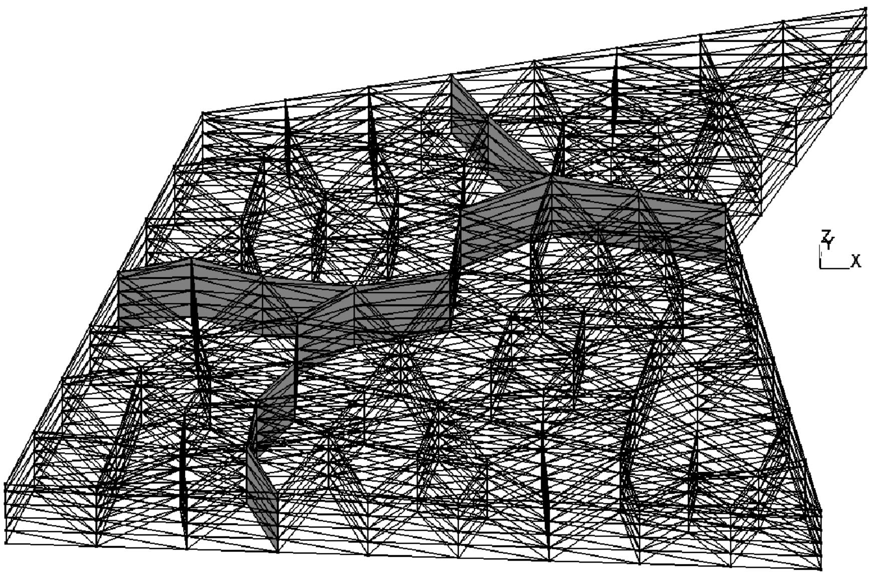

Fig. 1. The area and mesh of the test problems.

Figure 1), are homogeneous Neumann ones (meaning no flow through the boundary). On the front and back parts of the boundary, there the Dirichlet conditions are prescribed. The value of pressure there is prescribed due to z-coordinate so that the flow is induced just by the slope of the layers.

The second test problem is the same area without fractures, the permeability of the porous medium is higher so that at the same boundary conditions the inflow and outflow from the area are the same as in the first problem. The boundary conditions are the same.

Both computations were made on the mesh pictured at Figure 1 with 2271 tetrahedral elements. The fracture in the first problem was represented by 150 triangle mesh.

The resulting flow fields are noticeably different from each other. The flow through the fractured area (see Figure 2) is concentrated to the fracture. Almost no water flows elsewhere. It is not surprising since the permeability of fracture is 3 orders higher than permeability of porous medium. The flow field through purely porous medium area (see Figure 3) is very different, flow is distributed much more evenly in the whole area.

The difference in flow fields projects into dissolved species transport so that the propagation of contamination can be extremely overestimated or underestimated depending on the contamination source placement near or far from a fracture. This result demonstrates that if it is possible, the fractures in the modelled rock should be well localized and taken into account in modelling.

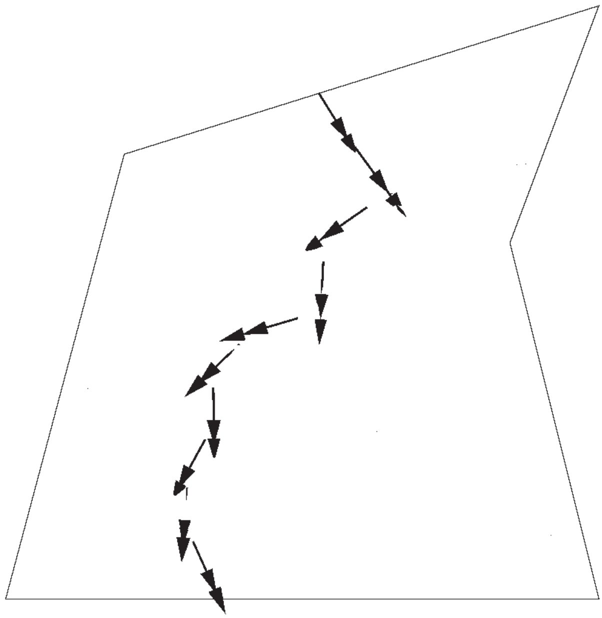

Fig. 2. Visualization of the computed flow field for the problem including fractures.

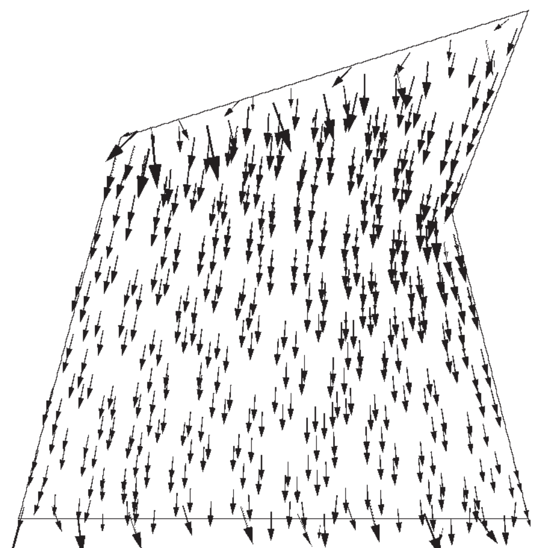

Fig. 3. Visualization of the computed flow field for the problem without fractures.

7. CONCLUSIONS

The presented formulation of water flow is based on connection of 1D, 2D, and 3D porous medium systems via the source terms only. It allows to construct meshes of the three systems independently on each other. It can save number of elements of constructed meshes, which saves computational time and allows to model large-scale real-world problems with less computational costs.

Actually, the model based on this formulation was implemented and it is a subject of testing at the time. The results of small-scale tests show qualitatively good behaviour of the model. The most recent open questions are the identification of σ_{ij} parameters in real problems and behaviour of the model in a large scale.

ACKNOWLEDGEMENT

This work was supported by the Ministry of Education, Youth and Sports of the Czech Republic under project number 1M4674788502, Research Centre Advanced Remediation Technologies and Processes.

(Received February 1, 2006.)

REFERENCES

[1] I. I. Bogdanov, V. V. Mourzenko, J. F. Thovert, and P. M. Adler: Effective permeability of fractured porous media in steady state flow. Water Res. Research *39* (2003), 1023–1038.

[2] D. M. Diodato: Compendium of Fracture Flow Models. Center for Environmental Restoration Systems, Energy Systems Division, Argonne National Laboratory, USA 1994. Available on: http://www.thehydrogeologist.com/docs/cffm/cffmtoc.htm.

[3] E. F. Kaasschieter and A. J. M. Huijben: Mixed-hybrid finite elements and streamline computation for the potential flow problem. Numer. Methods Partial Differential Equations *8* (1992), 221–266.

[4] J. Maryška: Approximation of the Mixed-hybrid Formulation of the Porous Media Flow Problem (in Czech). Technical Report No. 609, Institute of Computer Science of the Academy of Sciences of the Czech Republic, Prague 1995.

[5] J. Maryška, M. Rozložník, and M. Tůma: Mixed-hybrid finite-element approximation of the potential fluid-flow problem. J. Comput. Appl. Math. *63* (1995), 383–392.

[6] J. Maryška, M. Rozložník, and M. Tůma: Schur complement systems in the mixed-hybrid finite element approximation of the potential fluid flow problem. SIAM J. Sci. Comput. *22* (2000), 704–723.

[7] J. Maryška, O. Severýn, and M. Vohralík: Mixed-hybrid finite elements and streamline computation for the potential flow problem. Computational Geosciences *18* (2005), 8/3, 217–234.

[8] M. Vohralík, J. Maryška, and O. Severýn: Mixed and nonconforming finite element methods on a system of polygons. To appear in Appl. Numer. Math.

Jan Šembera, Jiří Maryška, Jiřina Královcová, and Otto Severýn, Technical University of Liberec, Hálkova 6, 461 17 Liberec. Czech Republic.

e-mails: jan.sembera@tul.cz, jiri.maryska@tul.cz, jirina.kralovcova@tul.cz, otto.severyn@tul.cz